Final version at JMMM 502, 15 May 2020, paper # 166568 https://doi.org/10.1109/JSEN.2020.3000442

Eddy Current Speed Sensor with Magnetic Shielding

Mehran Mirzaei, Pavel Ripka, Andrey Chirtsov, and Vaclav Grim

Faculty of Electrical Engineering, Czech Technical University, Prague 16627, Czech Republic
(e-mails: mirzameh@fel.cvut.cz, ripka@fel.cvut.cz)

***Abstract*—This paper presents the design and analysis of a new eddy current speed sensor with ferromagnetic shielding. Aluminum and solid iron are considered for the moving part. One excitation coil and two antiserially connected pick up coils are shielded by a thin steel lamination. 3D time stepping finite element analysis is used to analyze the sensor performance with different magnetic materials and compared with experimental results. The compactness, simplicity and excellent linearity with different magnetic materials for the moving part show uniqueness of the proposed speed sensor. The shielding increases sensitivity and reduces the influence of close ferromagnetic objects and interferences on the sensor performance.**

***Keywords*—Eddy current speed sensor, aluminum, iron, shielding, magnetic permeability and finite element method.**

I. Introduction

Speed sensors are vital parts of linear and rotating machines for control and protection purposes [1]-[3]. Contactless magnetic speed sensors are resistant against dust and oil, which brings them advantage over optical sensors [4]. The most popular sensor type is based on reluctance variation. Eddy current speed sensors work for all conducting moving bodies including those with smooth surface. They have simple construction and present favorable solution especially at high speeds. Longitudinal and perpendicular configurations of eddy current speed sensors and speed effects utilizations were presented in [5]-[11]. The presented models in [5] - [11] had only nonmagnetic aluminum moving part, which is simpler for analysis but not practical for industry in comparison with solid iron moving part. The authors analyzed and tested similar eddy current speed sensors for solid iron rod linear [12] and rotational configuration [13] without magnetic yoke and shield. These sensors suffered from sensitivity to magnetic interference and also to the presence of ferromagnetic materials from their vicinity. The magnetic shielding and magnetic yoke can increase the sensitivity of eddy current speed sensors as it provides low magnetic reluctance for the magnetic flux.

In this paper, a linear eddy current speed sensor with magnetic yoke and shielding using 0.5 mm silicon steel lamination is presented. Aluminum and solid iron moving bodies are both used in the finite element method (FEM) modeling and measurements. The effects of magnetic materials of the shielding are also investigated. Different excitation frequencies and speeds are considered in the measurements and analysis to obtain best sensor output linearity and sensitivity.

II. Eddy Current Speed Sensor

A. Model

Table I and Fig. 1 present the eddy current speed sensor model and parameters. Parameter, V is the speed in Fig. 1.

Table I
Eddy current speed sensor parameters

Parameters		Values
I	excitation coil current amplitude	166 mA
N	number of turn in all coils	100
L	moving part width	100 mm
h_m	moving part thickness	5.0 mm
h_c	coils thickness	4.7 mm
$w_{c,o}$	outer coil width	29.0 mm
$w_{c,i}$	inner coil width	25.0 mm
w_s	ferromagnetic shield width	30 mm
l_s	ferromagnetic shield length	90 mm
σ_{al}	moving part aluminum conductivity at room temperature	33.5 MS/m
σ_i	moving part solid iron conductivity at room temperature	6.0 MS/m
μ_{ri}	relative magnetic permeability of moving part solid iron	100
σ_s	silicon steel shield conductivity	3.1 MS/m
μ_{rs}	relative magnetic permeability of silicon steel shield	1000

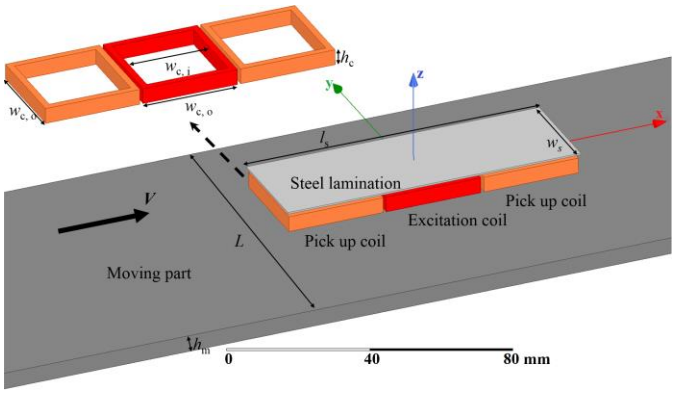

Fig. 1. Eddy current speed sensor with steel lamination for shielding

Final version at JMMM 502, 15 May 2020, paper # 166568 https://doi.org/10.1109/JSEN.2020.3000442

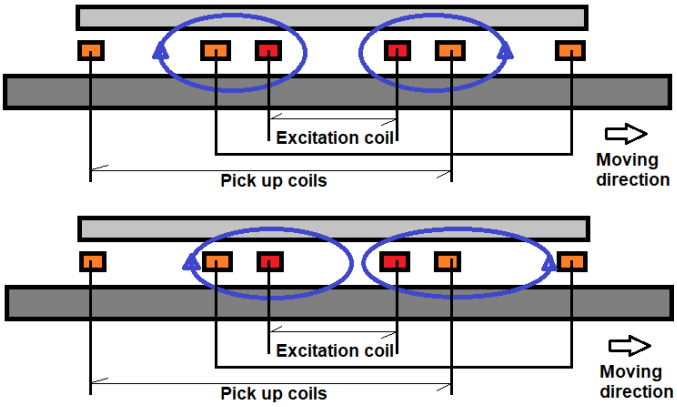

Fig. 2. 2D schematic models of eddy current speed sensor and moving part with single excitation coil and antiserially connected pick up coils – at zero speed (up) and nonzero speed (bottom)

B. *Operation Theory*

Two pick up coils (Fig. 1 and Fig. 2) are. Ideally induced voltage and net flux in the antiserially pick up coils are zero at zero speed because left and right side coils have same flux linkage with the excitation coil. The net total flux of antiserially connected pick up coils is nonzero at nonzero speed because pick up coils sense different flux linkages due to the induced eddy currents as shown in Fig. 2. The flux linkages of pick up coils are affected unevenly by motion component of induced eddy current [5], [14]. As speed increases, the difference between induced voltages of left and right side coils increases, which is utilized for the speed sensing for solid conductive moving objects.

III. Speed Sensor Measurements

A. *Experimental setup*

Experimental set up and measurement devices are shown in Fig. 3. A rotating disk (aluminum and iron) with thickness 5 mm is considered as moving part. The disk rotates between -500 rpm up to +500 rpm and center of eddy current speed sensor is located 22.5 cm distance from disk center. The dimensions of eddy current speed sensor are reasonably small in comparison with rotating disk therefore it can be assumed that eddy current speed sensor sense linear speed relative to the rotating disk. The electrical conductivities of iron and aluminum disk were measured and mentioned in Table I at room temperature. Lock-in amplifier is used for precise measurements of pick up coils voltage. A signal generator with internal resistance 50 Ω is connected to the excitation coil.

Fig. 3. Experimental set up – rotating disk (aluminum and solid iron) as moving part and eddy current based speed sensor (left) and signal generator and locked-in amplifier (right)

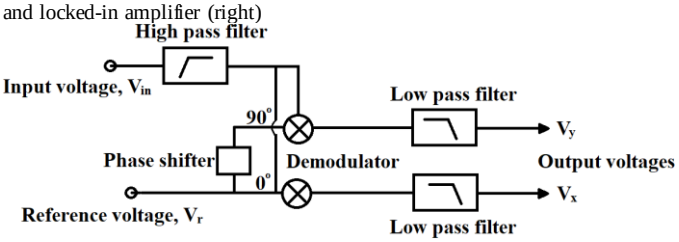

Fig. 4. Schematic block diagram to demonstrate the possible electronics diagram to process speed sensor output signal

Fig. 4 shows schematic block diagram, which can be considered for possible electronic design for the sensor.

B. *Speed sensor results*

Fig. 5 and Fig. 6 present measured absolute value of measured voltage, V_a of pick up coils:

$$V_a = \sqrt{V_r^2 + V_i^2} \quad (1)$$

where, V_r and V_i are real component and imaginary component of induced voltage in the antiserially connected pick up coils relative to the excitation coil current as reference signal. The polarity of absolute value of voltage is calculated using phase shift relative to the excitation coil current.

Pick up induced voltages for the iron rotating disk increase with increasing excitation coil frequency, which is different to the aluminium rotating disk. Linearity of induced voltage versus linear speed for iron rotating rod is the best at 300 Hz and it is the best between 120 Hz and 180 Hz for aluminium rotating disk. The gap between coils of eddy current speed sensor and rotating disk is about 6.25 mm, which is sufficient reasonable value for many industrial applications. High linearity of induced voltage curve versus speed makes the proposed sensor to be suitable device for speed measurement. The real component and imaginary component of induced voltages show different tendency versus speed (Fig. 7-Fig.8).

Final version at JMMM 502, 15 May 2020, paper # 166568 https://doi.org/10.1109/JSEN.2020.3000442

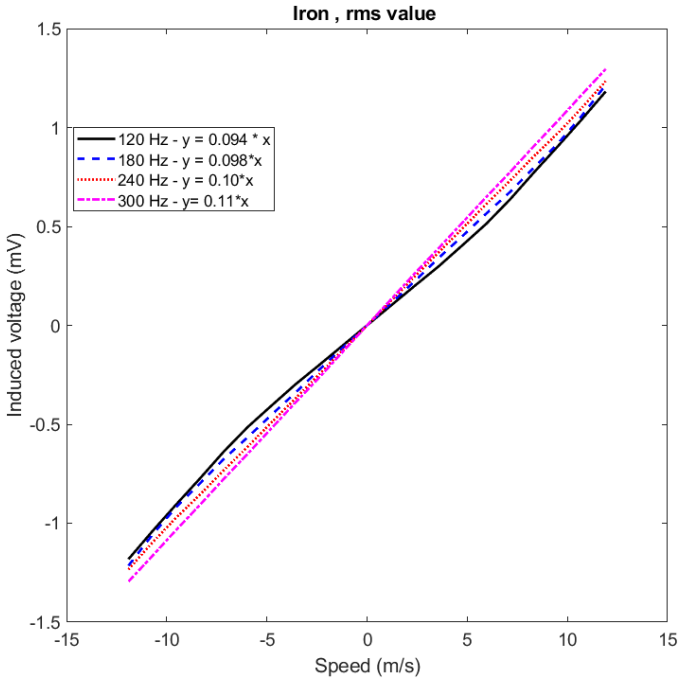

Fig. 5. Measured voltage of pick up coils for iron rotating disk at different frequencies – absolute value

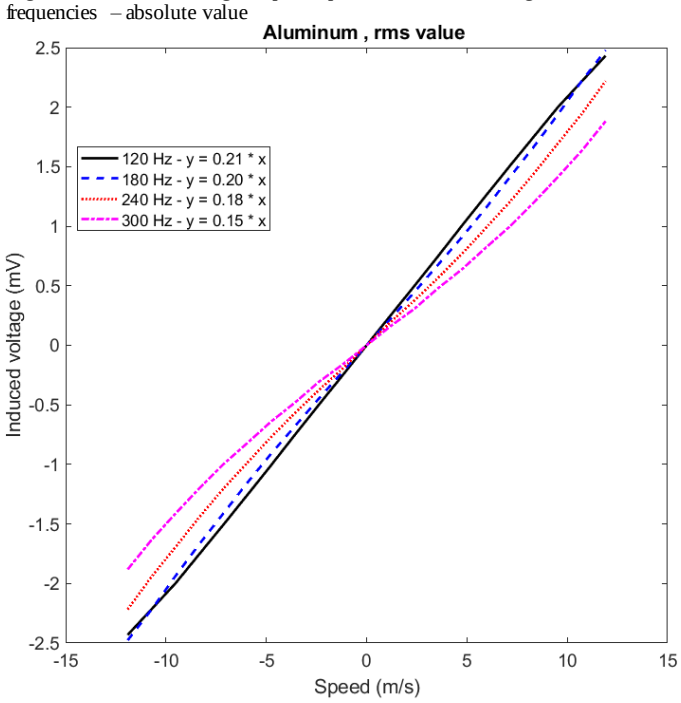

Fig. 6. Measured voltage of pick up coils for aluminum rotating disk at different frequencies – absolute value

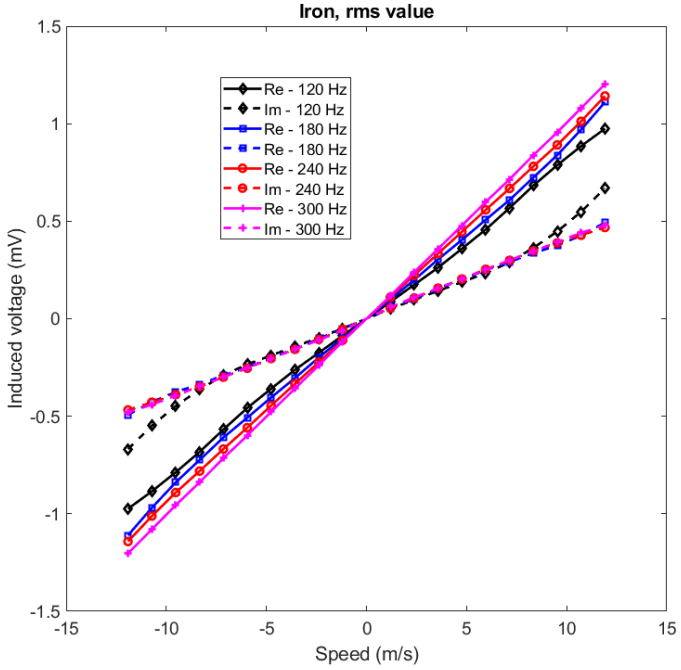

Fig. 7. Measured real component (Re) and imaginary component (Im) of induced voltage of pick up coils for iron rotating disk

Real component of induced voltage is more linear versus speed for all frequencies in comparison with imaginary component and its linearity is less dependent on the excitation frequency. Real component of induced voltage is proportional to the losses component in the rotating disk, which could be more reluctant to the speed sensor lift off.

It is shown that eddy current speed sensor sensitivity is highly dependent on the moving part material properties. Conductivity of aluminum and iron moving part and relative permeability of iron moving part could change eddy current speed sensor outputs [13]. Compensating moving part material properties on the eddy current speed sensor output is a challenging issue and it must be addressed.

The root mean square error (RMSE) for linearity in percentage value as an indicator [15] for representation of fitness of measured values to the linear curve fit is calculated about 0.26% for iron rotating disk at 300 Hz. Fig. 9 shows the error in percent of full range as an alternative approach for linearity error evaluation of speed sensor, which shows imaginary component of induced voltage is more linear than real component of induced voltage.

Final version at JMMM 502, 15 May 2020, paper # 166568 https://doi.org/10.1109/JSEN.2020.3000442

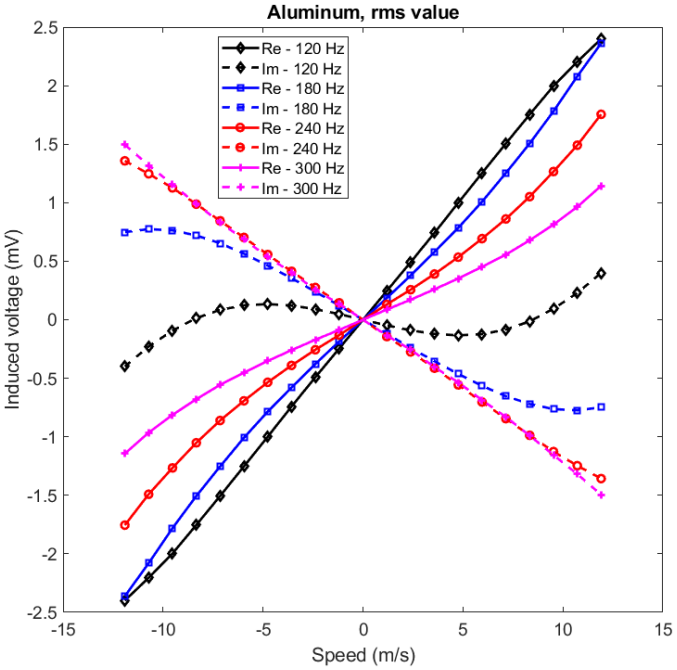

Fig. 8. Measured real component (Re) and imaginary component (Im) of induced voltage of pick up coils for aluminium rotating disk

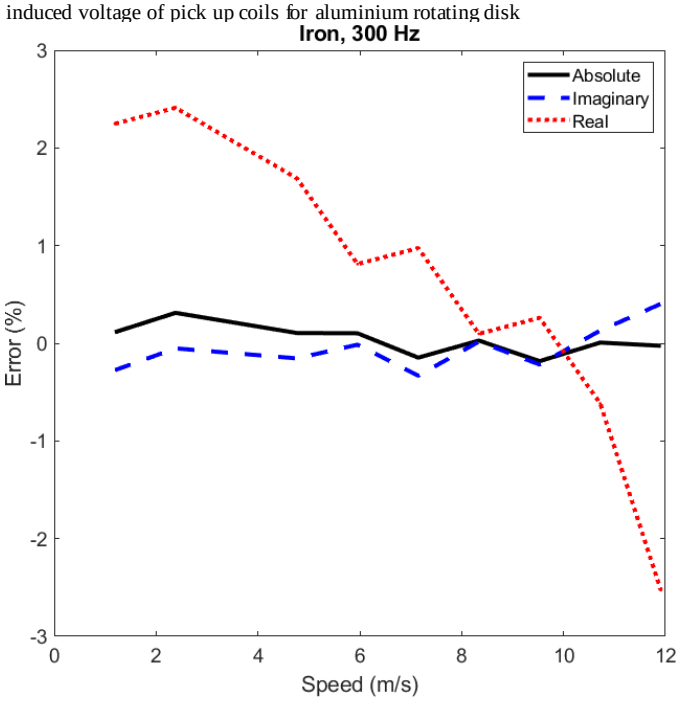

Fig. 9. Linearity error versus speed for absolute, imaginary and real components of induced voltages

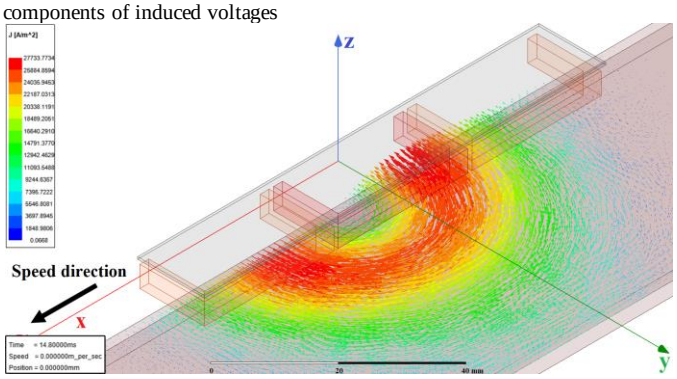

Fig. 10. Eddy current distribution in the aluminium moving part at zero speed

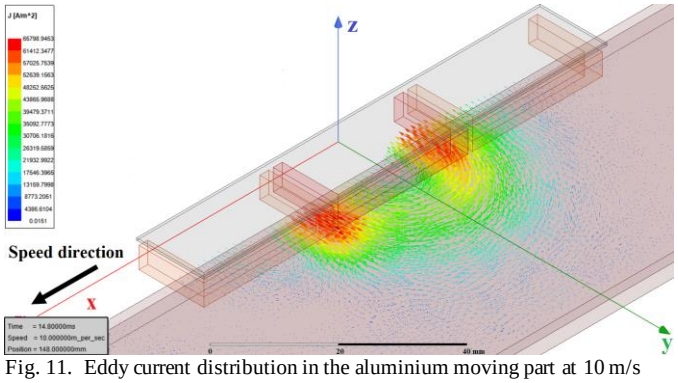

Fig. 11. Eddy current distribution in the aluminium moving part at 10 m/s

IV. 3D FEM Analysis

The performance of eddy current speed sensor is analyzed using time stepping 3D FEM tool [16]. The motion of moving part is considered at different speeds. Sliding mesh method is used in the FEM tool to model motion of moving part. The eddy current effects are taken into count in the shielding too as well as conductive moving part. In order to model accurately skin effects in the moving part and shielding, the mesh sizes are adjusted accordingly. Second order elements are utilized in the FEM tool, which high accuracy analysis could be achieved.

Only half of model is analyzed because of symmetry to save simulation time. Eddy current distribution in the aluminum moving part at zero speed and 10 m/s are shown in the Fig. 10 and Fig. 11. Eddy current distribution changes from symmetric form (Fig. 10) to asymmetric form (Fig. 11) due to the speed effect, which causes different induced voltage in the left and right side pick up coils.

A. *Comparison between Experiments and FEM*

Table II presents comparison between 3D FEM analysis and measurements at 2 m/s, 5 m/s and 10 m/s for aluminum and iron rotating disks. 3D FEM results coincide very well with measurements, which show accuracy of 3D FEM and its suitability for further steps, for example, eddy current speed sensor optimization and material effects evaluations.

Fig. 12 shows comparison between experimental and 3D FEM results versus time for rotating iron disk at 10 m/s.

Linear model is used for the simulation as sensor size and dimensions are very small in comparison with rotating disk. It is convenient to use disk or cylinder as a fine approximation for linear motion [17]-[20].

Final version at JMMM 502, 15 May 2020, paper # 166568 https://doi.org/10.1109/JSEN.2020.3000442

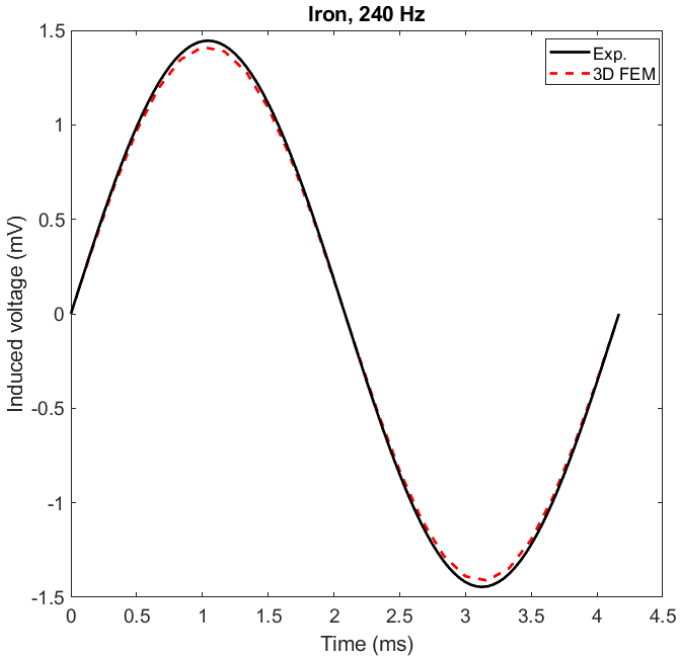

Fig. 12. Comparison between experimental and 3D FEM curves versus time at 10 m/s

Table II
Comparison between experimental results and FEM for induced voltage (mV) –rms value

	2 m/s Exp./ FEM	5 m/s Exp./ FEM	10 m/s Exp./ FEM
Aluminum 120 Hz	0.42/ 0.429	1.057/ 1.075	2.085/ 2.185
Aluminum 240 Hz	0.318/ 0.294	0.815/ 0.845	1.793/ 1.889
Iron 120 Hz	0.168/ 0.17	0.427/ 0.446	0.959/ 0.99
Iron 240 Hz	0.207/ 0.212	0.514/ 0.513	1.022/ 1.0

B. Ferromagnetic Materials Evaluation of Magnetic Shield and Moving Part

Table III presents effect of relative magnetic permeability of iron moving part on the sensor output. With increasing permeability the sensitivity is decreasing due to the decrease of penetration depth. Relative magnetic permeability varies for different steels and irons [21]-[22].

Effect of magnetic shielding is evaluated in the Table IV. First case is silicon steel with 0.5 mm thickness and estimated relative magnetic permeability 1000. The relative magnetic permeability in the second case is changed to 100, which induced voltage decreases considerably because of higher reluctance in the magnetic flux path. Third case is Ferrite core with 5 mm thickness and relative magnetic permeability 2000 for magnetic shielding, which induced voltage increases. However eddy current speed sensor becomes thicker and less compact.

Table III
FEM results of induced voltage (mV) for different moving part permeability – rms value

10 m/s	μ_{ri}=75	μ_{ri}=100	μ_{ri}=125
120 Hz	1.12	0.99	0.88
240 Hz	1.15	1.0	0.90

Table IV
FEM results of induced voltage (mV) for different magnetic shield materials – rms value

10 m/s 120 Hz	1- μ_{rs}=1000 σ_s=3.14 MS/m	2- μ_{rs}=100 σ_s=3.14 MS/m	3- μ_{rs}=2000 σ_s=0 MS/m
Iron	0.99	0.838	1.66
Aluminum	2.185	1.641	2.404

V. Conclusions

The proposed shielded eddy current speed sensor has sensitivity 110 µV/m/s for iron rotating disk at 300 Hz and 210 µV/m/s for aluminum rotating disk at 120 Hz. The 3D FEM calculations shows that shielding increases sensitivity by the factor over 2, but its main role is to suppress sensitivity to external magnetic fields and ferromagnetic objects. The linearity error is 0.26 % for iron moving part at 300 Hz.

The sensitivity can be increased several times by increasing number of turns of all coils; the limitations are the parasitic capacitances and shielding saturation.

The sensor can be optimized in terms of linearity and sensitivity using 3D FEM as the simulation results fits well with the measured values.

The sensor requires temperature compensation of the material properties and also compensation for the changes of lift-off: using ratiometric output V_1-V_2/(V_1+V_2) would be the first choice. This technique is successfully utilized in LVDT sensors. However, verification of such compensation is out of the scope of the present paper.

References

[1] C. Moron and E. Suarez, "Non-contact digital speed sensor," Journal of Magnetism and Magnetic Materials, 133, pp. 610-612, 1994

[2] C.-T. Liu, S.-Y. Lin, Y.-Y. Yang, C.-C. Hwang, "Analytical model development of an eddy-current-based non-contacting steel plate conveyance system," Journal of Magnetism and Magnetic Materials, 320, pp. 291–295, 2008

[3] Z. Zhang, C. Xi, Y. Yan, Q. Geng, T. Shi, "A hybrid analytical model for open-circuit field calculation of multilayer interior permanent magnet machines," Journal of Magnetism and Magnetic Materials, 435, pp. 136–145, 2017

[4] P. Ripka, *Magnetic Sensors and Magnetometers*, Artech House, Jan 1, 2001 - Technology & Engineering

[5] N. Takehira, and A. Tanaka, "Analysis of a perpendicular-type eddy-current speed meter," IEE Proc. A – Phys. Science, Meas. and Instr., Manag. and Educ.- Rev. , vol. 135 , no. 2, pp. 89 - 94, Feb. 1988

[6] T. Itaya, K. Ishida, A. Tanaka, N. Takehira, and T. Miki, "Eddy current distribution for a rectangular coil arranged parallel to a moving conductor slab," IET Science, Meas. & Tech., vol. 6, no. 2, pp. 43 - 51, Mar. 2012

[7] T. Itaya, K. Ishida, A. Tanaka, and N. Takehira, "Analysis of a fork-shaped rectangular coil facing moving sheet conductors," IET Science, Meas. & Tech. , vol. 3 , no. 4, pp. 279 - 285, Jul. 2009

[8] T. Itaya, K. Ishida, Y. Kubota, A. Tanaka, and N. Takehira, "Visualization of eddy current distributions for arbitrarily shaped coils parallel to a moving conductor slab," Progress In Electromagnetics Research M, Vol. 47, 1–12, 2016

[9] T. Itaya, K. Ishida, A. Tanaka, and N. Takehira, "Analysis of an eddy current speed meter by rectangular coil system," IEEJ Transactions on Fundamentals and Materials 133(8),416-423 , January 2013

[10] T. Itaya, K. Ishida, A. Tanaka, N. Takehira, and T. Miki, "Analysis of a fork-shaped rectangular coil oriented perpendicular to moving conductor slabs," NDT&E International, 44, 413–420, 2011

[11] A. Tuysuz, M. Flankl, J. W. Kolar, and A. Mutze, "Eddy-current-based contactless speed sensing of conductive surfaces," *IEEE 2nd Annual Southern Power Electronics Conference (SPEC)*, pp. 1 - 6, Dec. 2016
[12] M. Mirzaei, P. Ripka, A. Chirtsov, and J. Vyhnanek, "Eddy current linear speed sensor," IEEE Trans. Mag., vol. 55 , no. 1 , pp. 1-4, 2019
[13] M. Mirzaei, P. Ripka, J. Vyhnanek, A. Chirtsov and V. Grim, "Rotational eddy current speed sensor," IEEE Trans. Mag., (Early access) 2019
[14] T. C. Wang, "Linear induction motor for high-speed ground transportation," IEEE Transactions on Industry and General Applications, vol. IGA-7, no. 5, pp. 632-642, 1971
[15] H. Sumali, E.P. Bystrom, G.W. Krutz, "A displacement sensor for nonmetallic hydraulic cylinders," IEEE Sensors Journal, vol. 3, no. 6, pp. 818 - 826, 2003
[16] Ansys-Maxwell software, Accessed on 20.07.2019:https://www.ansys.com/products/electronics/ansys-maxwell
[17] O.C. Coho, G.B. Kliman, J.I. Robinson, "Experimental evaluation of a high speed double sided linear induction motor," IEEE Transactions on Power Apparatus and Systems, vol. 94, no. 1, pp. 10-18, 1975
[18] M. Iwamoto, S. Sakabe, K. Kitagawa, G. Utsumi, "Experimental and theoretical study of high-speed single-sided linear induction motors," IEE Proceedings B - Electric Power Applications, vol. 128, no. 6, pp. 306-312, 1981
[19] T. Haller, W. Mischler, "A comparison of linear induction and linear synchronous motors for high speed ground transportation," IEEE Transactions on Magnetics, vol. 14, no. 5, pp. 924-926 , 1978
[20] M. Iwamoto, E. Ohno, T. Itoh, Y. Shinryo, " End-Effect of High-Speed Linear Induction Motor," IEEE Transactions on Industry Applications, vol. IA-9, no. 6, pp. 632-639, 1973
[21] M. Lu, W. Zhu, L. Yin, A.J. Peyton, W. Yin and Z. Qu, "Reducing the lift-off effect on permeability measurement for magnetic plates from multifrequency induction data, " IEEE Transactions on Instrumentation and Measurement, vol. 67, no. 1, pp. 167 - 174, 2018
[22] M. Lu, R. Huang, W. Yin, Q. Zhao, A. Peyton, "Measurement of permeability for ferrous metallic plates using a novel lift-off compensation technique on phase signature," IEEE Sensors Journal, vol. 19, no. 17, pp. 7440 - 7446, 2019